A Combined Density Functional Theory and Molecular Mechanics (QM/MM) Study of Single-Site Ethylene Polymerization Catalyzed by $[(C_6H_5N{=}CH)C_4H_3N]_2\text{-}RM^+$ $\{M = Ti, Zr\}$ in the Presence of the Counterion $CH_3B(C_6F_5)_3^-$

Kumar Vanka, Zhitao Xu, and Tom Ziegler*

Department of Chemistry, University of Calgary, Calgary, Alberta, Canada T2N 1N4

Received December 4, 2003

Calculations have been carried out to investigate the insertion of the ethylene monomer into the M−methyl bond for the systems $[(C_6H_5N{=}CH)C_4H_3N]_2\text{-}CH_3M\text{-}\mu\text{-}CH_3\text{-}B(C_6F_5)_3$ (M = Ti and Zr), using density functional theory. Second insertion studies have also been conducted for the $[(C_6H_5N{=}CH)C_4H_3N]_2\text{-}C_3H_7Ti\text{-}\mu\text{-}CH_3\text{-}B(C_6F_5)_3$ system. A validated QM/MM model was used to represent the counterion. The C_6H_5 groups in the ligands were modeled with QM/MM, with hydrogens being used as the capping atoms. With R = Me (the initiation step), approach of the ethylene cis to the μ-Me bridge (cis approach) and from between the pyrrolide imine ligands (trans approach) were considered, along a path leading first to uptake of ethylene to form a π-complex followed by insertion of ethylene into the M−R bond. For the titanium-based system, the uptake was found to be rate determining for the cis approach, the total barrier being 12.9 kcal/mol, and the insertion barrier was found to be rate determining for the trans approach, the total barrier being 13.8 kcal/mol. For the zirconium-based system, the insertion barriers was rate determining for both cis and trans approaches, the total barriers being 9.4 and 10.6 kcal/mol, respectively. The propagation step was then studied for the contact ion-pair $[(C_6H_5N{=}CH)C_4H_3N]_2\text{-}C_3H_7Ti\text{-}\mu\text{-}CH_3\text{-}B(C_6F_5)_3$ (**4**). Different conformations of the propyl chain in **4** were considered by altering θ, the dihedral angle formed between the $C_\beta-C_\alpha-Ti$ and the $C_\alpha-Ti-\mu C$ planes. The resting states were found to be at $\theta = -80°$ (**4a**), $-180°$ (**4b**), and 40° (**4c**). A maxima was found near $\theta = 0°$ (**4d**). Cis and trans approaches of the ethylene monomer were considered for each of the four cases. All approaches of ethylene toward **4a** and **4c** conformers led to insertion, as did cis approach toward **4b** and trans approach toward **4d**. Uptake barriers were found to be rate determining for all the cis cases. The insertion barriers for all the trans cases of approach were uniformly higher than the corresponding cis barriers, by 5−10 kcal/mol. The lowest rate-determining insertion barrier was found for the uptake step for the cis approach in **4c**: 11.1 kcal/mol. Termination by hydrogen transfer from chain to monomer was found to occur for the cis approach of monomer toward **4d** and trans approach toward **4b**. The lowest termination barrier was higher than the lowest rate-determining insertion barrier by 6.3 kcal/mol.

I. Introduction

The field of olefin polymerization by single-site homogeneous catalysts has seen remarkable growth and development over the past twenty years.[1] The ability of single-site catalysts to achieve high stereoselectivity and narrow molecular weight distribution has made them emerge as viable alternatives to traditional Ziegler−Natta type heterogeneous catalysts.[2] The fact that they are structurally well-defined mononuclear active complexes has allowed the systematic modification of their structures for enhanced control over polymer properties. The state-of-the-art homogeneous catalysts transform simple alkenes into polymers with rate accelerations and stereo- and regiospecificities that rival those of enzymatic catalysts.

Among the more highly active homogeneous catalysts are metallocenes and related organometallic compounds containing a group IV transition metal. The general structure of these complexes consists of a group 4 transition metal center (M) coordinated to two ligands (L) and two methyl groups: L_2MMe_2. Bis-cyclopentadienyl (bis-Cp) complexes of the early transition metals are highly effective homogeneous olefin polymerization catalysts, but extensive patent coverage has spurred the development of new catalysts that do not contain the bis-Cp ligand framework.[3] Recently Yoshida et al.[4] have prepared titanium complexes with two pyrrolide imine

---

(1) (a) Resconi, L.; Cavallo, L.; Fait, A.; Piemontesi, F. *Chem. Rev.* **2000**, *100*, 1253. (b) Mashima, K.; Nakayama, Y.; Nakamura, A. *Adv. Polym. Sci.* **1997**, *133*, 1. (c) Alt, H. G.; Koppl, A. *Chem. Rev.* **2000**, *100*, 1205.

(2) *Metallocene-Catalyzed Polymers: Materials, Properties, Processing and Markets*; Benedikt, G. M., Goodall, B. L., Eds.; Plastic Design Library: New York, 1998.

10.1021/om034349h CCC: $27.50
Publication on Web 05/05/2004

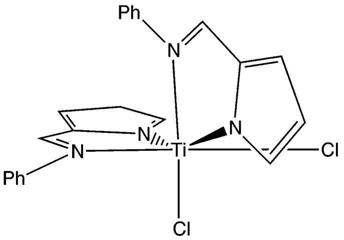

Figure 1. PI system: $[(C_6H_5N{=}CH)C_4H_3N]_2$-$TiCl_2$.

chelate ligands (henceforth referred to as the "PI" system) $[(C_6H_5N{=}CH)C_4H_3N]_2$-$TiCl_2$ (see Figure 1), which upon activation by MAO produced active polymerization catalysts. A modified version of these catalyst systems[5a] $[7$-$(RN{=}CH)C_8H_5N]_2$-$TiCl_2$ (R = phenyl and phenyl derivatives) exhibits the characteristics of living ethylene polymerization.

The process by which the cocatalyst can activate the complex is illustrated in Figure 2 below. First, a methyl group is extracted by the acidic cocatalyst compound denoted as "A" in the figure. This leads to a charge-separated contact ion-pair. The formation of this ion-pair species is exothermic, with the enthalpy of ion-pair formation denoted as ΔH_{ipf} in Figure 2. The ion-pair can finally separate into the active catalyst species and the anion, MeA^-. The energy required for a complete separation is denoted as ΔH_{ips}.

The mechanism for olefin polymerization, where the completely dissociated cation is considered as the active species, is shown in Figure 3 with ethylene as the olefin monomer.

The well-defined molecular structure of metallocene catalysts and their analogues has also enabled thorough mechanistic investigations by theoretical methods, and several theoretical studies[6] have been conducted, using the bare cation, L_2MR^+, as the model for the single-site catalyst. These studies have helped improve the understanding of the mechanistic aspects of the monomer insertion process. However, recent findings indicate[7] that the anionic counterion plays an important role in the polymerization process. Calculations showed[7e] that the value of ΔH_{ips} was very high, implying that the total dissociation of the contact ion-pair leading to formation of the bare cation would not take place. The counterion would therefore remain in the vicinity of the cation during the insertion process. Hence, the influence of the counterion has to be taken into account and the mechanism for the insertion has to be modified accordingly, as shown in Figure 4 below.

In the modified mechanism of Figure 4, the ethylene first approaches the contact ion-pair and binds to it, forming a weak olefin complex. The enthalpy of this complexation is denoted as ΔH_{c}. From this complexed state, the ethylene monomer then approaches the alkyl chain and attempts to insert into the metal−alkyl bond, leading to a four-centered transition state. The internal barrier of the reaction path, from the olefin complex to the transition state, is defined as ΔH_{ib}. The total barrier of the reaction is denoted as ΔH_{tot} and is the sum of ΔH_{c} and ΔH_{ib}.

Unfortunately, due to the size of the counterions, theoretical studies of the mechanism outlined in Figure 3, where the counterion is incorporated, are difficult and involve considerable computational effort. Hence few examples of such studies are found in the literature. Nifant'ev et al.[8] have studied ethylene insertion for the $Cp_2ZrEt^+A^-$ ($A^- = CH_3B(C_6F_5)_3^-$, $B(C_6F_5)_4^-$) systems. Lanza et al.[9a] have investigated olefin insertion into the Ti−CH_3 bond of the $H_2Si(C_5H_4)(^tBuN)TiCH_3$-$CH_3B(C_6F_5)_3$ ion-pair; Fusco[9b] and Bernardi[9c] studied the same process for $Cp_2(Ti/Zr)CH_3$-$Cl_2Al[O(Al(CH_3)_3$-$AlHCH_3]_2$ and $Cl_2TiCH_3(\mu\text{-}Cl)_2AlH_2$, respectively. Chan et al.[9d] have investigated the formation of ethylene-separated ion-pair complexes for ion-pairs formed between different catalysts and the counterion $B(C_6F_5)_3$-CH_3^-, as well as ethylene insertion[7e] into the Zr−CH_3 bond in the Cp_2ZrCH_3-μ-CH_3-$B(C_6F_5)_3$ system.

In earlier theoretical studies,[10] we investigated the insertion of the ethylene monomer into the methyl chain of different catalyst systems of the type $L_1L_2TiCH_3^+$, in the presence of the counterion. The counterion used for the purpose of the investigation was $B(C_6F_5)_3CH_3^-$. For the sake of computational expediency, a QM/MM model was used for the counterion. This allowed us to study a large number of different systems. In the QM/MM model, the perfluoro phenyl (C_6F_5) groups in $B(C_6F_5)_3$-CH_3^- were replaced with MM atoms, and Cl atoms are used to cap the QM system. Thus, $B(C_6F_5)_3CH_3^-$ was replaced with $BCl_3CH_3^-$ in the QM calculations. This model has been validated[10b] and will be employed to

---

[3] (a) Britovsek, G. P.; Gibson, V. C.; Waas, D. F. *Angew. Chem., Int. Ed.* **1999**, *38*, 429. (b) Liang, L.-C.; Schrock, R. R.; Davis, W. M.; McConville, D. H. *J. Am. Chem. Soc.* **1999**, *121*, 5797. (c) Baumann, R.; Stumpf, R.; Davis, W. M.; Liang, l.-C.; Schrock, R. R. *J. Am. Chem. Soc.* **1999**, *121*, 7822. (d) Guerin, F.; Stewart, J. C.; Beddie, C.; Stephan, D. W.; *Organometallics* **2000**, *19*, 2994. (e) Yue, N.; Hollink, E.; Guerin, F.; Stephan, D. W. *Organometallics* **2001**, *20*, 4424.

[4] Yoshida, Y.; Matsui, S.; Takagi, Y.; Mitani, M.; Nitabaru, M.; Nakano, T.; Tanaka, H.; Fujita, T. *Chem. Lett.* **2000**, 1270.

[5] (a) Matsugi, T.; Matsui, S.; Kojoh, S.; Takagi, Y.; Imoue, Y.; Nakano, T.; Fujita, T.; Kashiwa, N. *Macromolecules* **2002**, *35*, 4880. (b) Yoshida, Y.; Matsui, S.; Takagi, Y.; Mitani, M.; Nakano, T.; Tanaka, H.; Kashiwa, N.; Fujita, T. *Organometallics* **2001**, *20*, 4793. (c) Matsui, S.; Mitani, M.; Saito, J.; Tohi, Y.; Makio, H.; Matsukawa, N.; Takagi, Y.; Tsuru, K.; Nitabaru, M.; Nakano, T.; Tanaka, H.; Kashiwa, N.; Fujita, T. *J. Am. Chem. Soc.* **2001**, *123*, 6847. (d) Mitani, M.; Mohri, J.; Yoshida, Y.; Saito, J.; Ishii, S, Tsuru, K.; Matsui, S.; Furuyama, R.; Nakano, T.; Tanaka, H.; Kojoh, S.; Matsugi, T.; Norio, K.; Fujita, T. *J. Am. Chem. Soc.* **2002**, *124*, 3327.

[6] (a) Woo, T. K.; Margl, P. M.; Ziegler, T.; Blöchl, P. E. *Organometallics* **1997**, *16*, 3454. (b) Woo, T. K.; Margl, P. M.; Lohrenz, J. C. W.; Blöchl, P. E.; Ziegler, T. *J. Am. Chem. Soc.* **1996**, *118*, 13021. (c) Margl, P. M.; Lohrenz, J. C. W.; Blöchl, P. E.; Ziegler, T. *J. Am. Chem. Soc.* **1996**, *118*, 4434.

[7] (a) Yang, X.; Stern, C. L.; Marks, T. J. *J. Am. Chem. Soc.* **1994**, *116*, 10015. (b) Deck, P. A.; Marks, T. J. *J. Am. Chem. Soc.* **1995**, *117*, 6128. (c) Jia, L.; Stern, C. L.; Marks, T. J. *Organometallics* **1997**, *16*, 842. (d) Li, L.; Marks, T. J. *Organometallics* **1998**, *17*, 3996. (e) Chan, M. S. W.; Ziegler, T. *Organometallics* **2000**, *19*, 5182.

[8] Nifant'ev, I. E.; Ustynyuk, L. Y.; Laikov, D. N. *Organometallics* **2001**, *20*, 5375.

[9] (a) Lanza, G.; Fragala, I. L.; Marks, T. J. *Organometallics* **2002**, *21*, 5594. (b) Fusco, R.; Longo, L.; Masi, F.; Garbassi, F. *Macromol. Rapid Commun.* **1998**, *19*, 257. (c) Bernardi, F.; Bottoni, A.; Miscione, G. P. *Organometallics* **1998**, *17*, 16. (d) Chan, M. S. W.; Vanka, K.; Pye, C. C.; Ziegler, T. *Organometallics* **1999**, *18*, 4624. Vanka, K.; Ziegler, T. *Organometallics* **2001**, *20*, 905. (f) Zurek, E.; Woo, T. K.; Firman, T.; Ziegler, T. *Inorg. Chem.* **2001**, *40*, 361. (g) Zurek, E.; Ziegler, T. *Inorg. Chem.* **2001**, *40*, 3279. (h) Zurek, E.; Ziegler, T. *Organometallics*, accepted for publication.

[10] (a) Vanka, K.; Xu, Z.; Ziegler, T. *Isr. J. Chem.* **2002**, *42* (4), 403. (b) Xu, Z.; Vanka, K.; Firman. T.; Michalak, A.; Zurek, E.; Zhu, C.; Ziegler, T. *Organometallics* **2002**, *21*, 2444. (c) Xu, Z.; Vanka, K.; Ziegler, T. *Organometallics*, accepted for publication. (d) Ziegler, T.; Vanka, K.; Xu, Z. To be submitted. (e) Zurek, E.; Ziegler, T. *Faraday Discuss.* **2003**, *124*, 93. (f) Vanka, K.; Xu, Z.; Ziegler, T. *Can. J. Chem.*, accepted for publication. (g) Vanka, K.; Xu, Z.; Ziegler, T. *Macromol. Symp.*, accepted for publication. (h) Xu, Z.; Vanka, K.; Ziegler, T. *Macromol. Symp.*, accepted for publication.

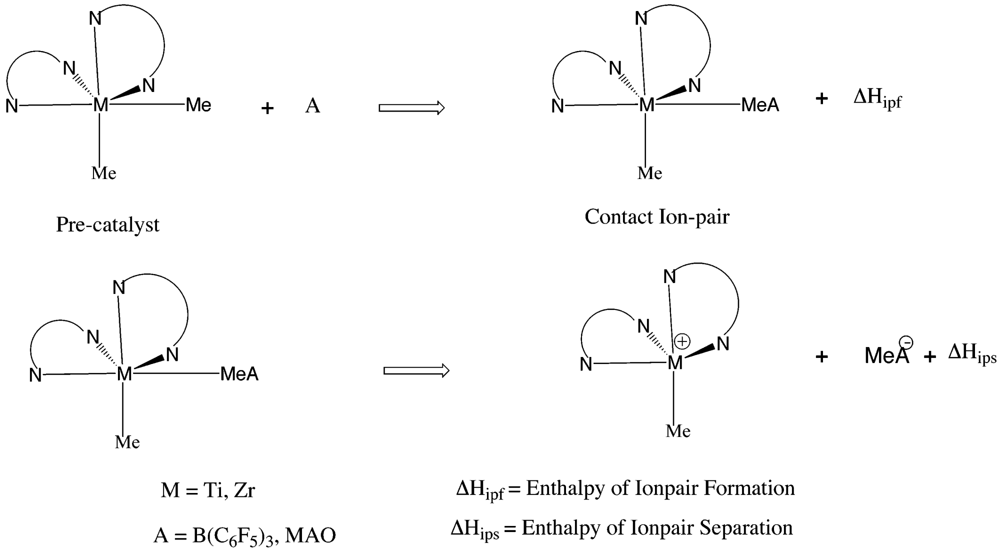

M = Ti, Zr

A = $B(C_6F_5)_3$, MAO

ΔH_{ipf} = Enthalpy of Ionpair Formation

ΔH_{ips} = Enthalpy of Ionpair Separation

Figure 2. Activation of the precatalyst by the cocatalyst.

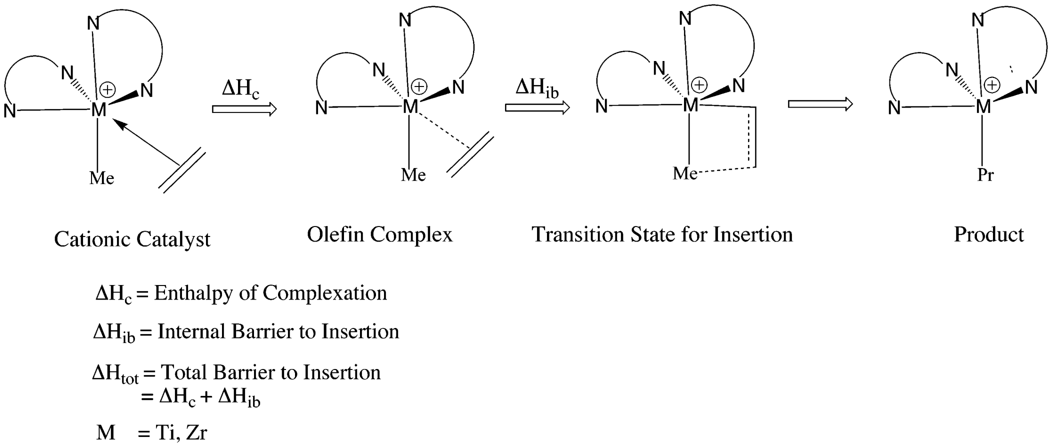

ΔH_c = Enthalpy of Complexation

ΔH_{ib} = Internal Barrier to Insertion

ΔH_{tot} = Total Barrier to Insertion
= $\Delta H_c + \Delta H_{ib}$

M = Ti, Zr

Figure 3. Mechanism for the complexation and insertion of the ethylene monomer into the metal–carbon bond of the cationic catalyst.

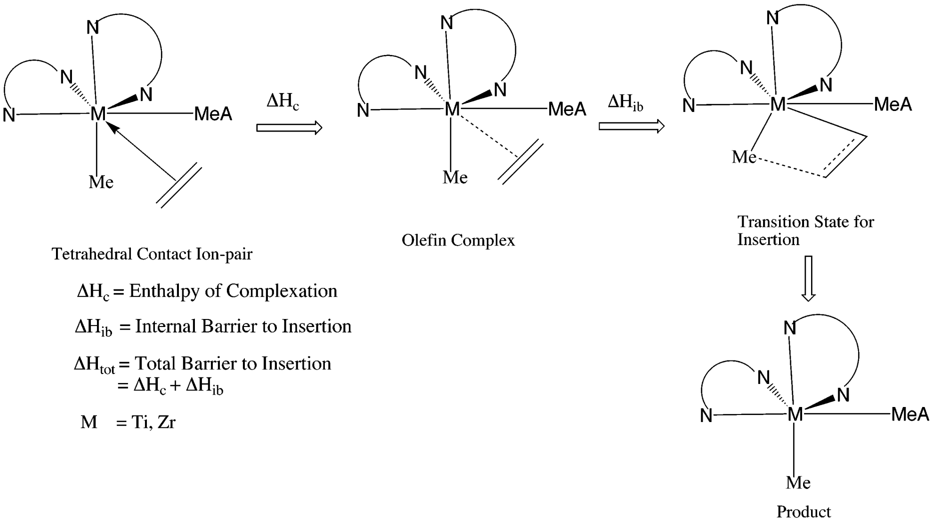

ΔH_c = Enthalpy of Complexation

ΔH_{ib} = Internal Barrier to Insertion

ΔH_{tot} = Total Barrier to Insertion
= $\Delta H_c + \Delta H_{ib}$

M = Ti, Zr

Figure 4. Mechanism of complexation and insertion of the ethylene monomer into the metal–carbon bond of the catalyst, in the presence of the counterion.

represent the $B(C_6F_5)_3CH_3^-$ counterion in the ion-pair systems studied in the present investigation.

In this present study, we investigate the approach of ethylene and its insertion into the Ti–methyl (initiation step) and Ti–propyl (propagation step) bonds for the $[(C_6H_5N{=}CH)C_4H_3N]_2$-RTi-$\mu$-$CH_3$-$B(C_6F_5)_3$ {R = CH_3 and C_3H_7} ion-pair systems. First insertion studies for the analogous zirconium-based system are also done for the purposes of comparison. Different approaches of the ethylene monomer toward the ion-pair will be considered for each case. Before the investigation of the propagation step, i.e., ethylene insertion into the propyl chain, different chain conformers of the free ion-pair will be considered to determine the most favorable conformation, prior to insertion.

The purpose of the investigation will be to isolate the important factors that contribute to the barrier of insertion and to compare and contrast the initiation and propagation steps for the same ion-pair system. The effect of the solvent on the insertion process will also be considered, with single-point solvation calculations to determine the energy of solvation for the ion-pair, the olefin complexes, and the transition states. Cyclohexane ($\epsilon = 2.023$) will be used as the solvent.

II. Computational Details

The density functional theory calculations were carried out using the Amsterdam Density Functional (ADF) program version 2000.01, developed by Baerends et al.[11] and vectorized by Ravenek.[12] The numerical integration scheme applied was developed by te Velde et al.,[13] and the geometry optimization procedure was based on the method of Verslius and Ziegler.[14] Geometry optimizations were carried out using the local exchange−correlation potential of Vosko et al.[15] without any symmetry constraints. The electronic configurations of the atoms were described by a triple-ζ basis set on titanium ($n = 3$) and zirconium ($n = 4$) for ns, np, nd, and (n+1)s, augmented with a single (n+1)p polarization function. Double-ζ STO bases were used for carbon (2s,2p), hydrogen (1s), and nitrogen (2s,2p), augmented with a single 3d polarization function except for hydrogen, where a 2p polarization function was used. Shells of lower energy were treated by the frozen core approximation. A set of auxiliary s, p, d, f, and g STO functions centered on all nuclei was used to fit the molecular density and represent Coulomb and exchange potentials accurately in each SCF cycle.[16] The gas phase energy difference was calculated by augmenting the local density approximation energy with Perdew and Wang's nonlocal correlation and exchange corrections (PWB91).[17] The solvation energies were obtained from a single-point full QM calculation using the conductor-like screening model (COSMO)[18] and optimized geometries from QM/MM calculations. A dielectric constant of 2.023 was used to represent cyclohexane as the solvent. The radii used for the atoms in Å were as follows: C 2.0, H 1.16, B 1.15, N 1.5, F 1.2, Ti 2.3, and Cl 2.1. Only the electronic contribution was calculated to evaluate the enthalpy of the reactions considered in this work. The enthalpies (ΔH) reported in the following sections are potential energy differences without zero-point corrections or vibrational finite temperature corrections. Such corrections are still too expensive to calculate for the size of molecules considered here. We expect these corrections to be on the order of ±2−3 kcal/mol. The insertion barriers were obtained by doing linear transit calculations for the same reaction coordinates, the C−C distance between one C of the ethylene and the C_α of the CH_3 or C_3H_7 groups, which represent the growing chains. The uptake barriers were obtained by doing linear transit calculations for the approach of the ethylene monomer toward the metal center of the ion-pair, with $\Delta R = R(\text{M}-\mu\text{-CH}_3) - R(\text{M}-\text{X})$ as the reaction coordinate, where M−μ-CH_3 represents the bond between the metal center and the carbon in the μ-methyl bridge, and M−X represents the bond between the metal center and the midpoint of the ethylene monomer. The MM atoms were described using the SYBYL/TRIPOS 5.2 force field constants.[19a] The code for QM/MM in ADF has been implemented by Woo et al.[19b]

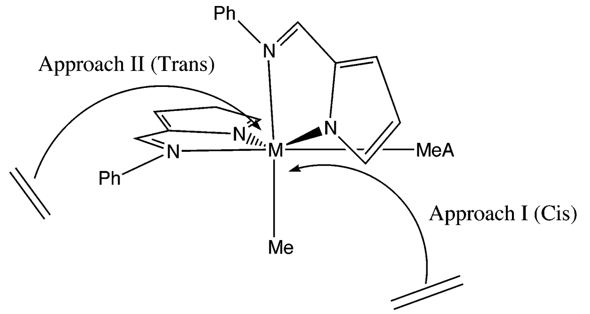

Figure 5. Different modes of approach of the ethylene monomer toward the contact ion-pair, $[(C_6H_5N{=}CH)\text{-}C_4H_3N]_2\text{-TiMe-}\mu\text{-MeB}(C_6F_5)_3$.

III. Results and Discussion

a. First Insertion Study with Inclusion of the Counterion. First insertion (initiation step) studies have been conducted for the real system $[(C_6H_5N{=}CH)\text{-}C_4H_3N]_2\text{-CH}_3\text{Ti-}\mu\text{-CH}_3\text{-B}(C_6F_5)_3$ (**1**) using MM (molecular mechanics) atoms to model the (C_6H_5) groups in the cation, with hydrogens as the capping atoms, and a validated QM/MM model[10b] (discussed in the Introduction) for the $B(C_6F_5)_3CH_3^-$ counterion. The barrier of uptake of the monomer, before the π-complex can be formed, and the barrier for insertion were calculated for different approaches of the ethylene monomer relative to the μ-methyl bridge of the contact ion-pair.

Figure 5 shows the different ways in which the ethylene monomer can approach the octahedral contact ion-pair. The most favorable approaches for the ethylene were found to be cis to the μ-methyl bridge (approach I in Figure 5) and approach II (Figure 5): an attack from between the pyrrolide imine groups. This approach is nearly trans to the μ-methyl bridge and will be referred to as the trans approach. The energy profiles for ethylene insertion from these two approaches will be discussed in the following sections.

(i) Cis Approach. The approach of the ethylene monomer cis to the μ-methyl bridge of the ion-pair, **1**, was studied using $\Delta R = R(\text{Ti}-\mu\text{-C}) - R(\text{Ti}-\text{X})$ as the reaction coordinate, where X is the midpoint of the C═C bond in the ethylene. Figure 6 shows the reaction profile for this approach. The energies reported in Figure 6 are solvent corrected, with gas phase values indicated in parentheses.

---

(11) (a) Baerends, E. J.; Ellis, D. E.; Ros, P. *Chem. Phys.* **1973**, *2*, 41. (b) Baerends, E. J.; Ros, P. *Chem. Phys.* **1973**, *2*, 52. (c) te Velde, G.; Baerends, E. J. *J. Comput. Phys.* **1992**, *92*, 84. (d) Fonseca, C. G.; Visser, O.; Snijders, J. G.; te Velde, G.; Baerends, E. J. In *Methods and Techniques in Computational Chemistry, METECC-95;* Clementi, E., Corongiu, G., Eds.; STEF: Cagliari, 1995; p 305.

(12) Ravenek, W. In *Algorithms and Applications on Vector and Parallel Computers*; te Riele, H. J. J., Dekker, T. J., van de Horst, H. A., Eds.; Elservier: Amsterdam, The Netherlands, 1987.

(13) (a) te Velde, G.; Baerends, E. J. *J. Comput. Chem.* **1992**, *99*, 84. (b) Boerrigter, P. M.; te Velde, G.; Baerends, E. J. *Int. J. Quantum Chem.* **1998**, *33*, 87.

(14) Verslius, L.; Ziegler, T. *J. Chem. Phys.* **1988**, *88*, 322.

(15) Vosko, S. H.; Wilk, L.; Nusair, M. *Can. J. Phys.* **1980**, *58*, 1200.

(16) Krijn, J.; Baerends, E. J. *Fit Functions in the HFS-Method*; Free University of Amsterdam, 1984.

(17) Perdew, J. P. *Phys. Rev. B* **1992**, *46*, 6671.

(18) (a) Klamt, A.; Schuurmann, G. *J. Chem. Soc., Perkin Trans.* **1993**, *2*, 799. (b) Pye, C. C.; Ziegler, T. *Theor. Chem. Acc.* **1999**, *101*, 396.

(19) (a) Clark, M.; Cramer, R. D., III; van Opdenbosch, N. J. Comput. Chem. **1989**, *10*, 982. (b) Woo, T. K.; Cavallo, L.; Ziegler, T. *Theor. Chim. Acta* **1998**, *100*, 307. (c) Maseras, F.; Morokuma, K. *J. Comput. Chem.* **1995**, *16*, 1170.

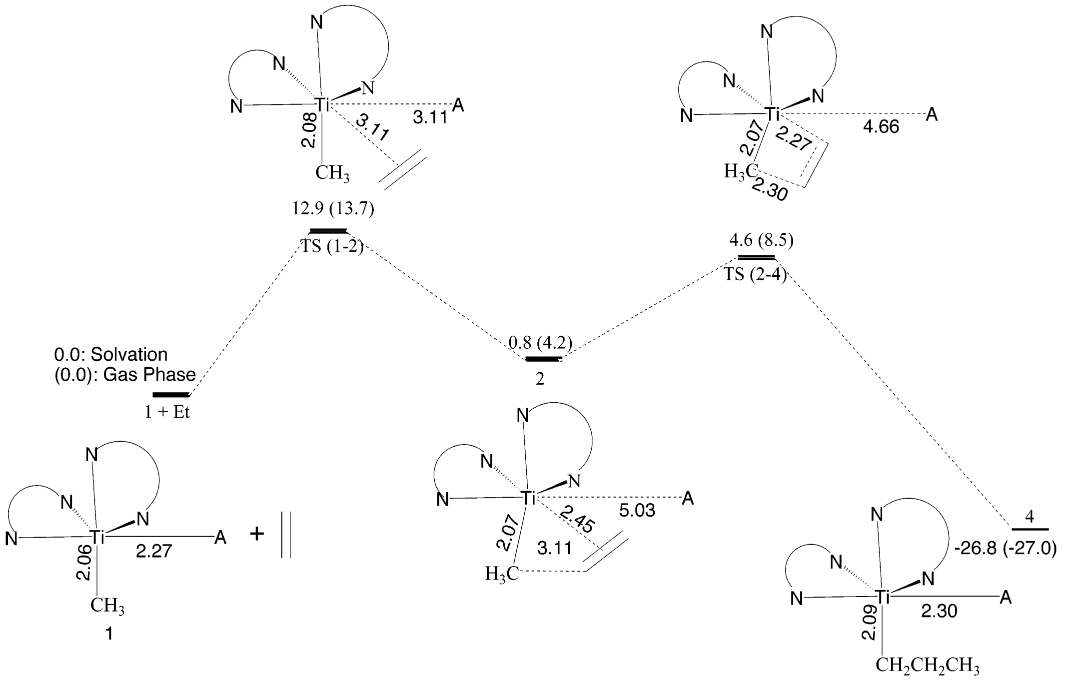

Figure 6. Energy profile for the cis approach of the ethylene monomer toward the contact ion-pair $[(C_6H_5N{=}CH)C_4H_3N]_2$-TiMe-$\mu$-$MeB(C_6F_5)_3$.

As the ethylene approaches the contact ion-pair, it displaces the counterion from the vicinity of the metal center. There is also increased steric congestion around the metal center due to its approach. There is an energy cost to the approach due to these factors, leading eventually to an uptake barrier of 12.9 kcal/mol. The ethylene is only bonding weakly to the titanium at this uptake transition state, **TS(1−2)**, being 3.11 Å away (see Figure 6), while the R(Ti−μ-C) distance has also increased, from 2.27 Å in the ion-pair **1** to 3.11 Å in **TS(1−2)**.

From here, the ethylene approaches the metal center and the counterion is further displaced, until the ethylene π-complex, **2**, is finally formed. The counterion has been considerably displaced at this stage, with R(Ti−μ-C) = 5.03 Å. However, despite the loss of bonding with the counterion, **2** is found to be only 0.8 kcal/mol higher in energy than **1**. The reason the system is so stable, despite the considerable displacement of the counterion, can be attributed to the ease with which the constituent ions can be separated in the PI systems. Full QM (quantum mechanical) calculations done on the model ion-pair system, $[(RN{=}CH)C_4H_3N]_2$-Ti-μ-CH_3-B-$(C_6F_5)_3$ (R = H), showed us that the energy required to completely separate the cation $[(HN{=}CH)C_4H_3N]_2$-$TiCH_3^+$ and the anion $B(C_6F_5)_3CH_3^-$ was 62.2 kcal/mol in the gas phase. This is about 15−20 kcal/mol lower than the bis-cyclopentadienyl and other catalyst systems.[10b] This ease of separation is due to the presence of four electron donating ancillary ligands on the metal center, in contrast to two for the bis-cyclopentadienyl and other nonmetallocenes. Hence, the displacement of the counterion to 5.03 Å comes at a lower cost of energy in comparison to the metallocene and other systems, while the metal center gets stabilization by π-complexation with the monomer. Moreover, the steric congestion around the metal center is also decreased with the displacement of the counterion, thereby stabilizing the system further. In addition, the influence of the solvent also comes into play due to the considerable charge separation between the cation and the anion, further stabilizing the system.

After formation of **2**, the ethylene approaches the Ti−Me bond, to enable the insertion to take place. This leads to an increase in energy and to the eventual formation of the four-centered insertion transition state, **TS(2−4)**, lying 4.6 kcal/mol higher than the separated reactants. The counterion is still considerably displaced, with R(Ti−μ-C) = 4.66 Å, while the $R(C_{monomer}-C_\alpha)$ distance has decreased to 2.3 Å. From **TS(2−4)**, the energy decreases as the C−C and Ti−propyl bond formations take place, until the final propyl chain product, **4**, is formed, at an energy of 26.8 kcal/mol below the separated reactants, **1** and ethylene (see Figure 6).

The energy profile for the cis approach, discussed above, shows the uptake barrier to be the rate-determining step. This is in contrast to the bis-cyclopentadienyl, constrained geometry and mono-cyclopentadienyl-ketimide systems,[10c,f] where, for the first insertion, the insertion step was found to be rate determining. The reason for this difference can be attributed to the difference in steric congestion at the metal coordination sphere between the PI system and the aforementioned systems: the PI system has four ancillary ligands around the metal center in contrast to two for the other systems. Therefore, steric factors become important when the ethylene approaches the metal center, therby increasing the steric congestion, with the counterion still not fully displaced, leading to a rise in energy. The insertion transition state lies lower in energy due to the greater ease of separation of the counterion, as discussed earlier.

The rate-determining barrier of 12.9 kcal/mol is comparable to the barriers obtained for the mono-cyclopentadienyl-ketimide and constrained geometry

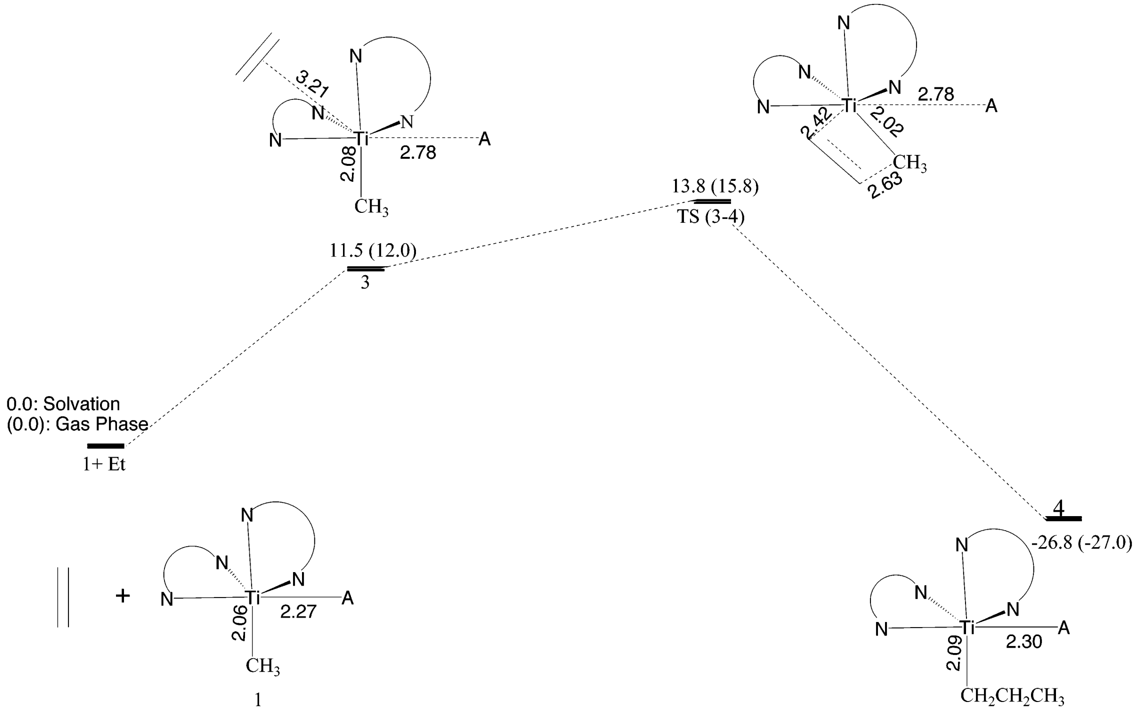

Figure 7. Energy profile for the trans approach of the ethylene monomer toward the contact ion-pair $[(C_6H_5N{=}CH)C_4H_3N]_2$-TiMe-$\mu$-MeB$(C_6F_5)_3$.

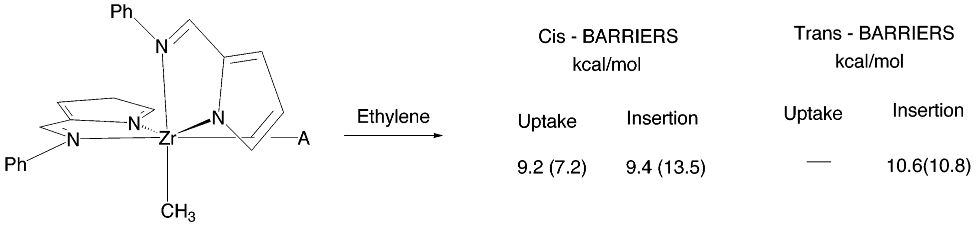

Figure 8. Uptake and insertion barriers for cis and trans approaches of the ethylene monomer toward the contact ion-pair $[(C_6H_5N{=}CH)C_4H_3N]_2$-ZrMe-$\mu$-MeB$(C_6F_5)_3$.

systems, which explains its experimentally observed activity.[4]

(ii) Trans Approach. The approach of the ethylene from between the pyrrolide imine groups was investigated next, and the energy profile is shown in Figure 7. The ethylene approaches the metal center of **1**, until it forms an adduct complex, **3**, at a distance of 3.21 Å from the titanium. The counterion has been slightly displaced at this point, with $R(\mathrm{Ti}{-}\mu\text{-C}) = 2.78$ Å. No barrier to uptake of the monomer was found. The energy of the system has risen to 11.5 kcal/mol at **3** and rises more with the further approach of the ethylene, until the four-centered insertion transition state, **TS(3−4)**, is formed, lying 13.8 kcal/mol higher than the reactants. The final, propyl chain product, **4**, is finally formed as in the cis approach, 26.8 kcal/mol below that of the reactants, **1** and ethylene.

The trans approach is found to present a higher barrier to insertion in comparison to the cis, thereby implying that the insertion would be likely to proceed via the pathway cis to the μ-methyl bridge of the ion-pair.

(iii) Investigating the Zirconium-Based PI System. The previous two sections dealt with the titanium-based PI system, $[(C_6H_5N{=}CH)C_4H_3N]_2$-$CH_3$Ti-$\mu$-$CH_3$-B$(C_6F_5)_3$ (**1**). Calculations for the first insertion of ethylene were also done for the corresponding zirconium-based catalyst, $[(C_6H_5N{=}CH)C_4H_3N]_2$-$CH_3$Zr-$\mu$-$CH_3$-B$(C_6F_5)_3$ (**2**). As before, MM atoms were used to model the C_6H_5 groups in the ancillary ligands, and the validated QM/MM model was used for the counterion. Analogous to the Ti-based system, the complete reaction profile for the cis and trans approaches of the ethylene monomer were studied. The results are summarized in Figure 8.

For the cis case, the insertion barrier was found to be rate determining, at 9.4 kcal/mol, slightly higher than the uptake, which was found to be 9.2 kcal/mol. This is in contrast to the Ti-based system, **1**, where the uptake was rate determining. The reason for this is the increased coordination space around the zirconium metal center, which decreases the steric congestion, and thereby decreases the barrier to uptake.

For the trans approach, the energy was found to increase until the insertion barrier of 10.6 kcal/mol was encountered, after which insertion took place with a lowering of energy. Analogous to the Ti-based system, the cis approach was found to be the more facile of the two, after the incorporation of solvent effects. There was considerable displacement of the counterion during the cis approach (>3.0 Å), while there was a relatively minor displacement for the trans case, of about 0.5 Å. This led to the solvent having a significant influence over the

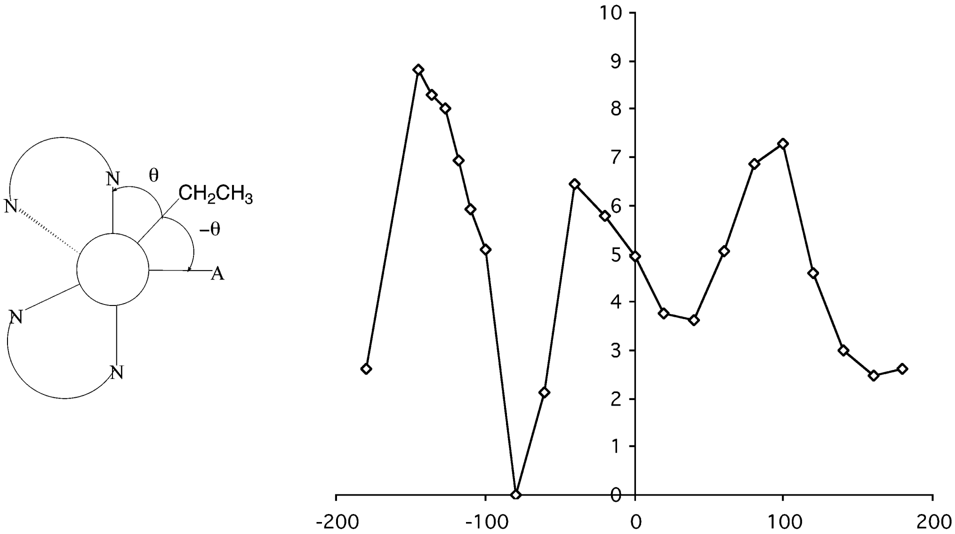

Figure 9. Relative stabilities of the different chain conformations formed by rotation of the propyl chain in the contact ion-pair $[(C_6H_5N{=}CH)C_4H_3N]_2$-TiPr-$\mu$-MeB$(C_6F_5)_3$.

rate-determining insertion step in the cis case, lowering the barrier in comparison to the other approach.

The rate-determining first insertion barrier of 9.4 kcal/mol for the favored cis approach is 3.5 kcal/mol lower than the corresponding rate-determining uptake barrier (12.9 kcal/mol) for the Ti-based PI system, **1**. The second insertion or propagation step of ethylene insertion was conducted only for the titanium-based PI system, but assuming that a similar trend favoring the zirconium-based systems is observed for the second insertion, the results suggest that the zirconium-based systems would perform as better catalysts than their Ti counterparts, if they can be synthesized and are stable under polymerization conditions.

b. Second Insertion Study with Inclusion of the Counterion. The resting state of the catalyst after the first insertion is the ion-pair: $[(C_6H_5N{=}CH)C_4H_3N]_2$-$C_3H_7$Ti-$\mu$-$CH_3$-B$(C_6F_5)_3$, i.e., the product formed at the completion of the first insertion, **4**. The second insertion or propagation step involves the approach and insertion of the ethylene monomer into the Ti−propyl chain of this ion-pair.

(i) Resting State of the Ion-Pair. In the ion-pair, formed after the first insertion, the alkyl group attached to the metal center has extended from a methyl to a propyl chain. This propyl chain can orient itself in several ways, to give rise to different conformations for the ion-pair. It is necessary to study these different conformations in order to determine the most stable resting state. This was done by a linear transit wherein the dihedral angle, θ, formed between the C_β−C_α−Ti and the C_α−Ti−μC planes was altered (see Figure 9 below) from −180° to 180° in order to rotate the chain so as to determine the most stable resting states. The accompanying energy profile in Figure 9 shows that the most stable resting states of the ion-pair correspond to the staggered conformations of the chain, with θ at −80°, 40°, and −180°, respectively. In contrast, the eclipsed conformations, with θ near −145° and θ at 0°, were found to be energy maxima. The rotation of the chain from $\theta = -80°$ to $\theta = -145°$ (eclipsed conformation) leads to an increase in energy of 8.8 kcal/mol. This represents the barrier to rotation of the propyl chain. Figure 9 also shows the relative energies of the different possible conformations.

For the insertion studies, four different conformations of the propyl chain were considered, with $\theta = -80°$ (**4a**), −180° (**4b**), 40° (**4c**), and 0°(**4d**). They correspond to the three minimum energy conformations of the ion-pair, **4a** ($\theta = -80°$), **4b** ($\theta = -180°$), and **4c** ($\theta = 40°$) as well as the maxima for θ near 0°, **4d**. The conformers **4a** and **4c** are the "out-of-plane" conformers, where the β and γ carbons of the propyl chain lie out of the plane formed by the α carbon, the metal center, and the μC bridge. By the same token, conformers **4c** and **4d** will be considered the "in-plane" conformers.

Beginning with the ion-pair in these four conformations, the approach of the ethylene monomer cis and trans to the μ-methyl bridge was studied. The results of the investigations are discussed below. The relative energies of the olefin complexes and insertion barriers were calculated with respect to the totally separated species: ethylene monomer and **4a**, the most stable conformation of the ion-pair in its resting stage.

The approach of the olefin monomer toward the ion-pair can lead to one of two possible outcomes: (a) insertion of the monomer resulting in the extension of the alkyl chain or (b) termination of the polymerization reaction by chain transfer from the alkyl chain to the monomer. In the next two sections (sections ii and iii), we will look at the first of the two possibilities—insertion—for the different orientations of the propyl chain. Both cis and trans cases of approach will be considered. Following that, in section iv we will investigate the other possibility—termination—for the different approaches.

(ii) Profile for the Most Favorable Insertion Pathway. Of all the pathways studied, the most facile approach was found for the cis attack of the monomer toward the ion-pair in orientation **4c**, i.e., with the propyl chain lying out of the plane formed by the α carbon, the metal center, and the μC bridge, with θ = 40°. Figure 10 shows the energy profile for this attack. The approach of the ethylene toward **4c** entails an energy expenditure of 11.1 kcal/mol, which is the uptake barrier that the system has to overcome before the

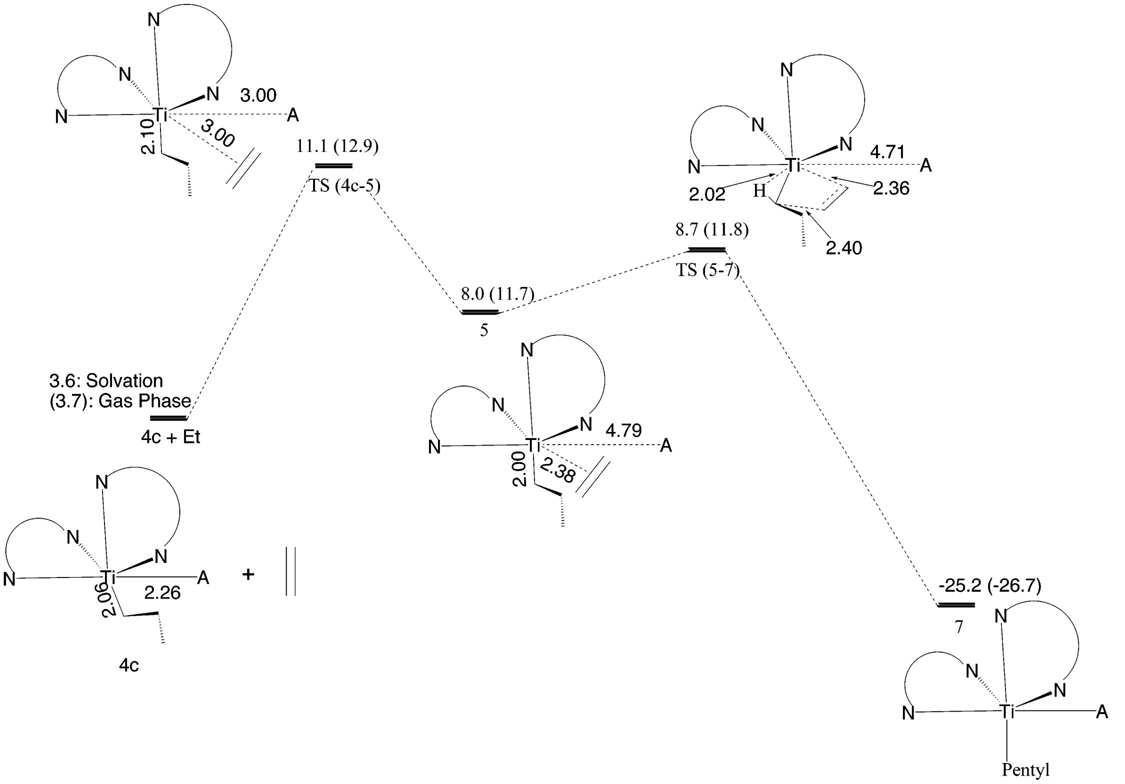

Figure 10. Energy profile for the cis approach of the ethylene monomer toward the contact ion-pair $[(C_6H_5N{=}CH)C_4H_3N]_2$-TiPr-$\mu$-MeB$(C_6F_5)_3$ for the case **4c**.

π-complex, **5** (see Figure 10), can be formed. At the uptake transition state, **TS(4c-5)** (see Figure 10), the ethylene still lies 3.00 Å away from the titanium metal center, while the counterion has been displaced by about 0.75 Å. From this point on, the counterion is displaced to a greater extent, as the ethylene moves in toward the titanium, but the energy of the system drops due to stabilization gained by the increased bonding between the titanium and the ethylene. The π-complex, **5**, is finally formed with the ethylene about 2.4 Å away from the metal center and the counterion displaced by about 2.5 Å. Solvent effects are substantial at this point, due to the large separation between the cation and the counterion, and the π-complex lies 8.0 kcal/mol above the separated reactant species. The insertion transition state, **TS(5−7)**, follows thereafter with only a slight increase in energy, to 8.7 kcal/mol. An agostic interaction exists at this transition state between one of the hydrogens on the α carbon of the chain and the metal center. After overcoming **TS(5−7)**, the ethylene begins to insert into the propyl chain to yield the pentyl chain product, **7**, lying 25.2 kcal/mol below the separated reactant species.

Hence the rate-determining step for this most facile approach of the monomer is the uptake step, with the barrier calculated to be 11.1 kcal/mol. This is 1.8 kcal/mol lower than the lowest rate-determining barrier for the first insertion case (12.9 kcal/mol) for the titanium-based PI system. This reduction in barrier upon going from first to second insertion is consistent with experimental observations[20] and calculations[10c,f] done previously on constrained geometry and mono-cyclopentadienyl ketimide systems.

(iii) Overall Picture for the Insertion for the Different Conformations. The cis and trans approaches were studied for all the other conformations of the ion-pair as well, and the results are collected in Figure 11.

All approaches of the ethylene monomer toward the “out-of-plane” conformers **4a** ($\theta = -80°$) and **4c** ($\theta = 40°$) were found to lead to insertion (see Figure 11). Also, insertion occurred for the cis attack in the case of the “in-plane” conformer **4b** ($\theta = -180°$) and for the trans approach of the monomer toward **4d** ($\theta = 0°$). The other two possibilities for the two in-plane chain conformations, i.e., trans attack toward **4b** and cis approach toward **4d**, led to termination and will be discussed later in section iv.

Figure 11 shows the uptake and insertion barriers for the different modes of attack. The chief features of the insertion processes are discussed in the four points below:

(i) For all approaches cis to the μ-methyl bridge, the insertion process shows the same characteristics as in the case of the first insertion, viz., the uptake barrier is found to be the rate-determining step. The displacement of the counterion is less at the uptake stage, with $R(\text{Ti}-\mu\text{-C}) \approx 2.8-3.0$ Å, and hence the steric congestion contributes to the higher uptake barriers. At the insertion stage, the $R(\text{Ti}-\mu\text{-C})$ has increased to about 4.8−5.0 Å, and the ethylene has more room near the metal center; the insertion barriers are consequently lower. Also, the stabilizing solvent effects are more significant.

(ii) For all approaches from between the pyrrolide imine groups leading to insertion, i.e., the trans approach of the monomer toward the “out-of-plane” **4a** and **4c** and the “in-plane” **4d**, the insertion barriers were

---

[20] Liu, Z.; Somsook, E.; White, C. B.; Rosaaen, K. A.; Landis, C. R. *J. Am. Chem. Soc.* **2001**, *123*, 11193.

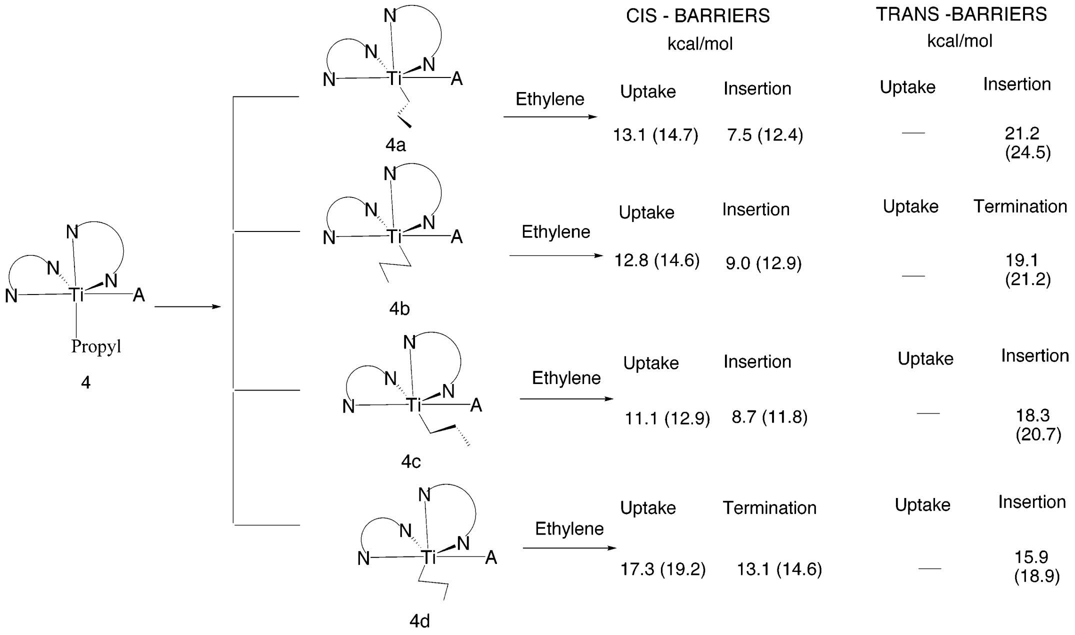

Figure 11. Overall picture of the second insertion step. The barriers obtained from the cis and trans approaches of the ethylene monomer toward the contact ion-pair $[(C_6H_5N{=}CH)C_4H_3N]_2$-TiPr-$\mu$-$MeB(C_6F_5)_3$, with the propyl chain in different conformations.

found to be 21.2, 18.3, and 15.9 kcal/mol, respectively. They were, therefore, higher than the corresponding cis uptake barriers by 5−10 kcal/mol (see Figure 11). It was, therefore, considered unnecessary to calculate the uptake barriers for these cases, as it was clear from the insertion barriers that the ethylene showed a marked preference for the cis pathway for insertion. This difference between the barriers is greater than observed for different modes of attack in the constrained geometry and mono-cyclopentadienyl-ketimide systems,[10c,f] indicating that the titanium-based PI system was more selective than the other catalysts studied. This is due to the greater steric hindrance that the ethylene has to contend with when it approaches the ion-pair from between the pyrrolide imine ligands (trans approach). As seen in Figure 5, the ethylene monomer avoids interaction with the bulky phenyl ligands when it approaches cis to the μ-methyl bond. However, in the trans cases of attack, such interactions are unavoidable and therefore increase the strain on the system, thereby destabilizing it.

(iii) For the “in-plane” cases, the four-centered insertion transition state showed a stabilizing agostic interaction between one of the hydrogens on the β-carbon of the propyl chain and the titanium, analogous to transition states observed in the “backside” insertions in theoretical studies of naked cations,[6] and of ion-pair systems.[10c,f] For the “out-of-plane” cases, there existed an α agostic interaction between a hydrogen of the α carbon of the propyl chain and the metal center, as observed for similar approaches in other systems.[10c,f]

(iv) As discussed in section ii, the lowest rate-determining barrier (11.1 kcal/mol) was found in the case of the uptake for the “out-of-plane” complex **4c** (see Figure 10), in line with similar results obtained for the constrained geometry and mono-cyclopentadienyl-ketimide systems in earlier investigations.

(iv) Termination for the Different Conformations. As seen from Figure 11, cis approach toward the “in-plane” conformer **4d** and trans approach toward in-plane **4b** lead to termination of the insertion process. The energy profile for the trans approach toward **4d** is discussed in Figure 12. The uptake barrier is the rate-determining step, with the uptake transition state **TS(4d-6)** occurring at 17.3 kcal/mol above the reactant species. The π-complex, **6**, is subsequently formed, lying 3.4 kcal/mol above the reactants. At this stage, a β agostic interaction exists between one of the hydrogens on the β carbon of the chain and the metal center. From here onward, in order for insertion to occur, the β carbon of the chain would have to rotate out of the plane so as to allow the ethylene to approach the α carbon of the chain. However, this rotation was found to have a prohibitively high barrier (>20 kcal/mol). The chain prefers, instead, to transfer a β hydrogen to the in-plane ethylene, leading to a hydrogen transfer transition state (**TS 6−8**) (see Figure 12), lying 11.1 kcal/mol above the separated reactants. The insertion process is thus terminated. The system stabilizes from that point onward to yield the final product **8**, with an ethyl chain and a propylene coordinated to the metal center. **8** is 4.2 kcal/mol more stable than the reactant species.

The trans approach toward the in-plane conformer **4b** also leads to termination, as seen from the data in Figure 11. The barrier for hydrogen transfer was calculated for this case to be 19.1 kcal/mol (see Figure 11).

Overall, the lowest rate-determining barrier to termination was determined to be 17.3 kcal/mol (see Figures 11 and 12), which is 6.3 kcal/mol higher than the lowest rate-determining barrier to insertion (see Figures 10 and 11). Therefore, the titanium-based PI system studied here would prefer insertion to termination. However, this difference of 6.3 kcal/mol is lower than that calculated for the constrained geometry and the mono-cyclopentadienyl-ketimide systems, studied earlier,[10c,f] where the difference between the insertion and termination barriers was about 10 kcal/mol. Hence

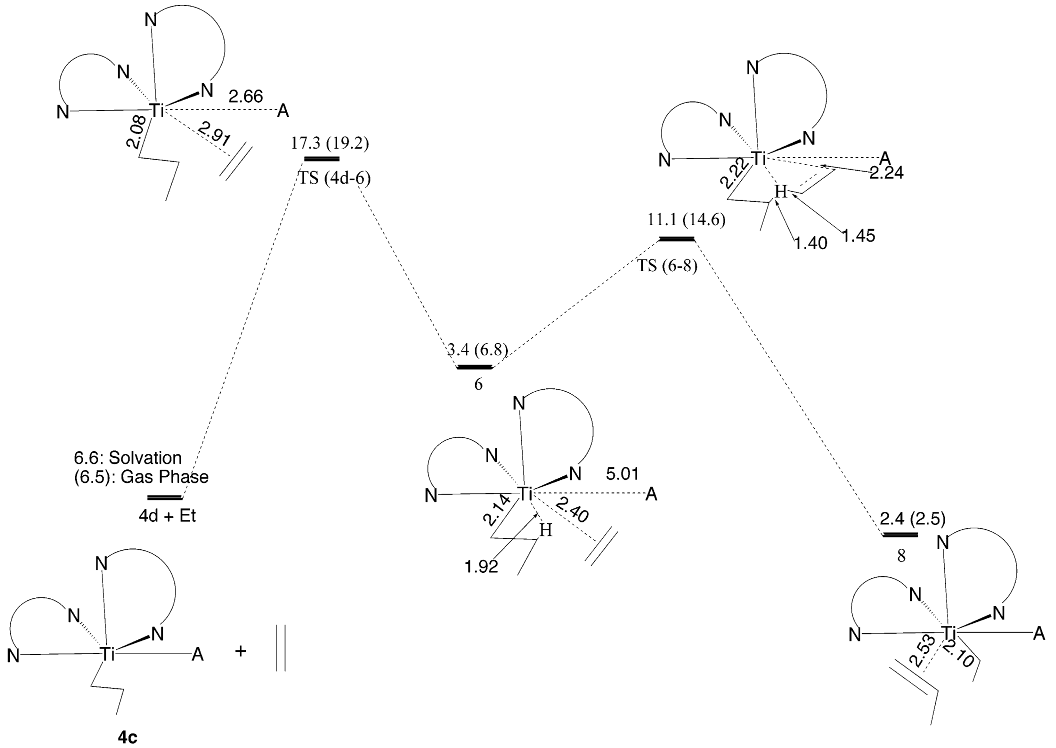

Figure 12. Energy profile for the cis approach of the ethylene monomer toward the contact ion-pair $[(C_6H_5N{=}CH)C_4H_3N]_2$-TiPr-$\mu$-$MeB(C_6F_5)_3$ for the case **4d**.

the titanium-based PI system, with $B(C_6F_5)_3CH_3^-$ as the counterion, is likely to yield lower molecular weights during ethylene polymerization, in comparison to the constrained geometry and the mono-cyclopentadienyl-ketimide systems.

Living ethylene polymerization has been experimentally observed for certain systems similar to the ones investigated in the current study.[5d] It was observed that the substitution of fluorine atoms in the ortho positions of the aryl rings bound to the imine nitrogens led to the living polymerization of ethylene. This "ortho-F" effect reflects similar results obtained with the use of bulky substituents on the chelating nitrogen atoms in the Brookhart[21] and McConville[22] catalysts. This has been theoretically examined[23] for the naked cationic Brookhart and McConville catalysts, and it was shown that the increase in steric bulk on the chelating nitrogens destabilized the six-centered chain transfer transition state (analogous to **TS(6−8)**, Figure 12) more than the compact four-centered insertion transition state (analogous to **TS(5−7)**, Figure 10). This explained the increase in molecular weight or living olefin polymerization observed in these systems. This effect has also been observed for Ziegler−Natta systems.[24] The "ortho-F" effect may therefore have a similar explanation. However, the incorporation of the counterion in the calculations, as is done in the current studies, shows that the uptake barriers for termination and insertion (**TS(4d−6)** and **TS(4c−5)**, respectively) are significant and are the respective rate-determining steps for the two processes. It would be interesting, therefore, to determine if the increase in the steric bulk on the chelating nitrogens affects the uptake barriers to a greater extent than the subsequent insertion or transfer barriers. This is currently being investigated.[25]

IV. Conclusions

A density functional study was conducted on the approach and insertion of the ethylene monomer into the Ti−C_α bond (C_α representing the first carbon of the alkyl chain) for the ion-pair $[(C_6H_5N{=}CH)C_4H_3N]_2$-RM-$\mu$-$CH_3$-$B(C_6F_5)_3$ (R = methyl, propyl; M = Ti, Zr): the "PI" system. QM/MM atoms were used to model the C_6H_5 groups in the ancillary ligands, with hydrogens used as capping atoms. The counterion, $B(C_6F_5)_3CH_3^-$, was represented by a previously validated QM/MM model.[10b] The chief conclusions from the study are summarized below:

(i) The presence of four ancillary ligands at the titanium metal center was seen to have the dual effect of (a) facilitating the displacement of the counterion by providing increased electron density at the metal center and (b) increasing the steric congestion at the metal coordination sphere. These effects serve to make the uptake barrier the rate-determining step in the insertion processes, for both the first and second insertions.

(ii) The selectivity of the cis approach over the trans is increased in the case of the PI system, in comparison to the constrained geometry and mono-cyclopentadienyl-ketimide systems.[10c,f]

---

(21) Ittel, S. D.; Johnson, L. K.; Brookhart, M. *Chem. Rev.* **2000**, *100*, 1169.

(22) Scollard, J. D.; McConville, D. H. *J. Am. Chem. Soc.* **1996**, *118*, 10008.

(23) (a) Deng, L.; Margl, P.; Ziegler, T. *J. Am. Chem. Soc.* **1997**, *119*, 1094. (b) Deng. L.; Woo, T. K.; Cavallo, L.; Margl, P. M.; Ziegler, T. *J. Am. Chem. Soc.* **1997**, *119*, 6177. (c) Deng. L.; Ziegler, T.; Woo, T. K.; Margl, P. M.; Fan, L. *Organometallics* **1998**, *17*, 3240. (d) Woo, T. K.; Ziegler, T. *J. Organometallic Chem.* **1999**, *591*, 204.

(24) Seth, M.; Ziegler, T. *Macromolecules* **2003**, *36*, 6613.

(25) Vanka, K.; Ziegler, T. Work in progress.

(iii) The zirconium-based systems gave lower first insertion barriers in comparison to the titanium-based systems. Second insertion studies were not done for the zirconium-based PI system, but the evidence of the first insertion indicates that they would be better catalysts if they can be synthesized and are stable under polymerization conditions.

(iv) The second insertion was found to be more facile than the first for the titanium-based PI system investigated, corroborating experimental[20] and theoretical[10c,f] evidence of the same.

Acknowledgment. This investigation was supported by the Natural Science and Engineering Research Council of Canada (NSERC) and by Mitsui Chemicals. T.Z. would like to thank the Canadian Government for a Canada Research Chair.

Supporting Information Available: The optimized geometries of the structures reported (Cartesian coordinates, in Å). This material is available free of charge via the Internet at http://pubs.acs.org.

OM034349H